

Theory of inelastic confinement-induced resonances due to the coupling of center-of-mass and relative motion

Simon Sala and Alejandro Saenz

AG Moderne Optik, Institut für Physik, Humboldt-Universität zu Berlin, Newtonstrasse 15, 12489 Berlin, Germany

(Dated: September 11, 2018)

A detailed study of the anharmonicity-induced resonances caused by the coupling of center-of-mass and relative motion is presented for a system of two ultracold atoms in single-well potentials. As has been confirmed experimentally, these inelastic confinement-induced resonances are of interest, since they can lead to coherent molecule formation, losses, and heating in ultracold atomic gases. A perturbative model is introduced to describe the resonance positions and the coupling strengths. The validity of the model and the behavior of the resonances for different confinement geometries are analyzed in comparison with exact numerical *ab initio* calculations. While such resonances have so far only been detected for large positive values of the *s*-wave scattering length, it is found that they are present also for negative *s*-wave scattering lengths, i. e. for attractive interactions. The possibility to coherently tune the resonances by a variation of the external confinement geometry might pave the way for coherent molecule association where magnetic Feshbach resonances are inaccessible.

I. INTRODUCTION

Theoretical treatments of strongly-correlated ultracold atoms in single-well potentials routinely adopt the harmonic approximation to describe the trapping potential. This is, of course, an idealization, because every realistic trapping potential is finite and thus anharmonic. A major benefit of a harmonic confinement is that for identical particles relative (rel.) and center-of-mass (c.m.) motion decouple. Moreover, especially for deep potentials the harmonic confinement resulting from a second-order Taylor expansion of the potential in its minimum might be a good approximation, especially since the center-of-mass to relative motion (c.m.-rel.) coupling introduced by the anharmonicity of the trapping potential is energetically negligible compared to the energy scale of the interatomic interaction. As a consequence, the theoretically predicted binding energy of two ultracold atoms confined in a harmonic trap [1] has been experimentally confirmed [2]. Moreover, the measurement [3] and calculation [4] of the influence of the anharmonicity on the energy of states in deep optical lattices has revealed that the deviation to the harmonic approximation for the lowest band is negligible in most cases.

On the first glance, it was therefore surprising that c.m.-rel. coupling can have a significant impact on an ultracold atomic quantum gas. In [5, 6] it was revealed that the particle loss and heating observed in [7] was caused by inelastic confinement-induced resonances (CIR), i. e. resonances due to the c.m.-rel. coupling of a c.m. excited bound state with an unbound atom pair – even in a deep optical lattice where the harmonic approximation has proven accurate for the rel. motion energies. The explanation of the losses due to *inelastic* CIR was necessary in order to resolve contradicting results of the experiment [7] and the theory of *elastic* CIR [8, 9] that originally was used as an explanation for the observed atom losses. Additionally, alternative explanations of the experimental findings were proposed based on the assumption of a harmonic confinement. One is based on multichannel ef-

fects [10], others [7, 11] on a Feshbach-type mechanism. Finally, in [12] it was demonstrated by simultaneously observing both the elastic and the inelastic CIRs and by excluding other mechanisms like many-body effects due to the design of the experiment that a coherent molecule formation is triggered uniquely at a c.m.-rel. coupling resonance which confirms the explanation of the losses in [7] in terms of the inelastic CIR. This demonstrates the importance of the anharmonicity-induced c.m.-rel. coupling, especially in view of its universality.

In fact, very recently it was demonstrated that inelastic CIR are also present in ultracold dipolar systems [13], and even for Coulomb-interacting systems such as excitons in quantum-dot systems [14]. For the latter, the resonances were proposed to serve as a novel kind of controlled single-photon source. At the inelastic CIR a variation of the exciton confinement leads to a redistribution of the charge density with subsequently increased annihilation probability of the electron-hole pair. Since this process can be steered *in situ* by a variation of the external confinement, single photons can be emitted on demand.

Resonances in atomic gases due to c.m.-rel. coupling have been mentioned in literature before. The first work explicitly discussing a possible molecule formation due to anharmonicity-induced c.m.-rel. coupling is [15]. In the model in [15] a deep isotropic optical lattice is considered. The evaluation of the c.m.-rel. coupling matrix elements is performed with wavefunctions in the harmonic approximation. A direct loss process is considered where two unbound atoms couple to a molecule in the continuum, i. e. the c.m.-part of the bound state is assumed to be a highly excited c.m. wavefunction which is approximated by a spherical wave. The work concludes that the dimer-production rate is too small to be significant in an optical-lattice experiment. The observed losses in [7] proof different, however, i. e. losses at inelastic CIR in a deep optical lattice are observed. The reason for the small dimer-production rate in [15] is that the coupling to highly excited bound states is very small as will be

shown in this work. On the other hand, as demonstrated in [5, 12], losses at inelastic CIR occur dominantly due to the coupling of a rel.-motion bound state with low-order c.m. excitation and subsequent three-body collisions, in contrast to a direct coupling to a rel.-motion bound state in the c.m. continuum as assumed in [15].

Even in a harmonic confinement a coupling of the c.m. and rel. motion is present in the case of heteronuclear atoms or identical atoms in different electronic states [16–18]. Moreover, the occurrence of Feshbach-type resonances due to the c.m.-rel. coupling was discussed in [19], their behavior in a superlattice was characterized in [20]. In mixed dimensions, the experiment performed in [21] also detected inelastic loss resonances for a variation of the scattering length. The behavior of the elastic and inelastic CIR within a quasi-1D lattice model was considered in [22].

In the present work, the two-body model that was introduced in [5] for the description of the positions of the resonances in quasi-1D and quasi-2D confinement observed in [7] is generalized to describe the position and coupling strength of in principle all c.m.-rel. coupling resonances in single-well potentials of arbitrary symmetry. The validity of the model is discussed in comparison to *ab initio* calculations. Resonance positions and coupling strengths are investigated for a change in the confinement geometry, i. e. in the transition between an almost isotropic to a cigar-shaped (quasi-1D) confinement and in the transition between an almost isotropic to a pancake-shaped (quasi-2D) confinement. It is demonstrated that higher-order resonances occur also for negative values of the *s*-wave scattering length. Consequently, by analyzing the wavefunction of the system it will be demonstrated that molecule formation also occurs in the strongly attractive interaction regime.

The paper is organized as follows: In Section II the two-body Hamiltonian is introduced and the basic idea of inelastic CIR is briefly recapitulated. Then a model is formulated to predict the position (Section III) and coupling strength (Section IV) of c.m.-rel. resonances. To validate the model, the behavior of the resonances is discussed under a varying geometry of the confining potential in Sections V and VI. Section VII deals with the optimization of c.m.-rel. coupling and the limitations of the model. It is then concluded in Section VIII that resonances ignored in previous considerations (e. g. in [5]) should also lead to a molecule formation in the strongly attractive interaction regime of ultracold atoms. The article closes with a conclusion in Section IX.

II. THE HAMILTONIAN

In c.m. and rel. coordinates, $\mathbf{r} = \mathbf{r}_1 - \mathbf{r}_2$ and $\mathbf{R} = \frac{1}{2}(\mathbf{r}_1 + \mathbf{r}_2)$, respectively, the Hamiltonian of two identical particles in an external trapping potential can be written

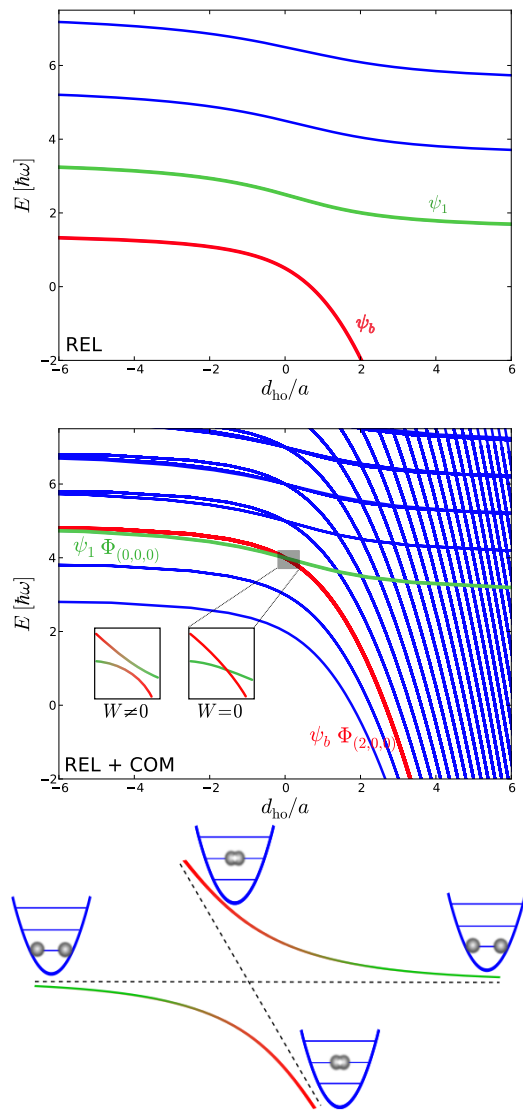


Figure 1. (Color online) Eigenenergy spectrum of two ultra-cold atoms in an isotropic harmonic trap interacting via a δ pseudopotential [1, 23] for a varying *s*-wave scattering length a (or varying confinement length d_{ho} which would, however, also change ω continuously). The upper panel shows the energy of the rel. motion Hamiltonian H_{rel} , the lower one the combined energy of the rel. and the c.m. motion Hamiltonians, i. e. $H_{rel} + H_{cm}$. Introducing a coupling between the rel. and c.m. motion makes the crossings avoided as illustrated in the lower part as solid lines, while the black dashed lines indicate the diabatic curves. Passing through the crossing adiabatically (on the solid line) allows for a transformation of the bound state with c.m. excitation into a trap state in the c.m. ground state.

as

$$H(\mathbf{r}, \mathbf{R}) = H_{rel}(\mathbf{r}) + H_{cm}(\mathbf{R}) + W(\mathbf{r}, \mathbf{R}) \quad (1)$$

$$H_{rel}(\mathbf{r}) = T_{rel}(\mathbf{r}) + V_{rel}(\mathbf{r}) + U_{int}(r) \quad (2)$$

$$H_{cm}(\mathbf{R}) = T_{cm}(\mathbf{R}) + V_{cm}(\mathbf{R}) \quad . \quad (3)$$

where T_{rel} and T_{cm} denote the kinetic-energy operators of the rel. and c.m. motion, respectively, and V_{rel} and V_{cm} are the separable parts of the potential energy. Thus, W contains only the non-separable terms of the potential energy. $U_{\text{int}}(r)$ is the interparticle interaction.

In Fig. 1 the eigenenergy spectrum of the Hamiltonian in Eq. (1) for two ultracold atoms interacting via the δ pseudopotential

$$U_{\text{int}}(r) = \frac{4\pi\hbar^2 a}{m} \delta(\mathbf{r}) \frac{\partial}{\partial r} r \quad , \quad (4)$$

a being the s -wave scattering length and m the atomic mass, is shown. The atoms are confined in an isotropic, i. e. spherically symmetric, harmonic trapping potential. The energies are plotted for a varying inverse s -wave scattering length d_{ho}/a , $d_{\text{ho}} = \sqrt{\frac{2\hbar}{m\omega}}$ being the harmonic oscillator length. The spectrum of H_{rel} (Eq. (2)) contains a bound state $|\psi_b\rangle$ bending down to negative infinity for $a \rightarrow 0^+$ and trap states, the energetically lowest one denoted as $|\psi_1\rangle$. In case of a harmonic trapping potential, the coupling W between the c.m. and the rel. motion vanishes. Hence, in order to obtain the spectrum of the full Hamiltonian (Eq. (1)) the c.m. energies are added to each state of the rel. spectrum, resulting in the middle plot of Fig. 1. Each state of the rel. spectrum appears now with an infinite series of c.m. excitations. Crossings appear between c.m. excited bound states, e. g., $|\psi_b\Phi_{(2,0,0)}\rangle$, and trap states, e. g., the lowest trap state $|\psi_1\Phi_{(0,0,0)}\rangle$. Introducing a coupling $W(\mathbf{r}, \mathbf{R}) \neq 0$ between c.m. and rel. motion turns the crossings to avoided ones (besides modifying the energies of the states also globally) and enables an adiabatic transition of a c.m.-excited molecular state and a state of an unbound atom pair in the c.m. ground state as indicated in the lower plot of Fig. 1.

Therefore, the c.m.-rel. coupling introduces a Feshbach-type resonance at the crossing position. The occupation of the bound state at the resonance is only possible because the excess binding energy can be transferred into c.m. excitation energy due to the anharmonicity of the confining potential. This redistribution of binding energy to kinetic energy marks an inelastic process and thus these c.m.-rel. coupling resonances were denoted as *inelastic* CIR. In [12] it is demonstrated how a coherent molecule formation can be realized at the c.m.-rel. coupling resonance. Such a molecule formation can trigger particle loss and heating in a many-body system in a two-step process. At the resonance two atoms coherently couple to the c.m.-excited molecular state. Then, this molecule collides either with another molecule or an unbound atom leading to a deexcitation of the molecule into a deeply bound state and subsequent loss of the involved particles from the trap.

The full two-body spectrum Fig. 1 shows a plethora of crossings. A full six-dimensional treatment of the two-body problem involving the c.m.-rel. coupling is possible [4, 24], but numerically quite demanding. Since c.m.-rel. coupling resonances can have a substantial influence on

the stability of an ultracold atomic gas, the knowledge of the position and coupling strength of the resonances is of great interest. The understanding and assignment of these resonances is in particularly important for an unbiased identification of other few-body resonances of, e. g., Efimov type. Therefore, simplified models that allow for the estimate of resonance positions and widths are desirable.

III. C.M.-REL. COUPLING MODEL – RESONANCE POSITIONS

A model is introduced to predict the position and coupling strength of the inelastic CIR. The theory generalizes the model described in [5] that is only applicable to strongly anisotropic (quasi-1D or quasi-2D) confinement and does not consider coupling strengths explicitly [25].

Of course, for c.m.-rel. coupling resonances to be present a c.m.-rel. coupling must be introduced. Therefore, the harmonic approximation has to be abandoned. Optical-lattice potentials [26] are widely used in ultracold experiments and offer a great degree of flexibility and control. In a deep optical lattice, i. e. $\frac{E_r}{V} \ll 1$ where $E_r = \frac{\hbar^2 k^2}{2m}$ is the recoil energy and V is the lattice depth, tunneling between neighboring wells is suppressed and the potential can be regarded as a stack of single-well potentials. In this work, a sextic potential is used resulting from a Taylor expansion of a \sin^2 optical-lattice potential up to the sixth degree. A separation of the expansion in rel., c.m., and coupling terms

$$V_{\text{rel}}(\mathbf{r}) = \sum_{j=x,y,z} V_j \left[\frac{1}{2} k_j^2 r_j^2 - \frac{1}{24} k_j^4 r_j^4 + \frac{1}{720} k_j^6 r_j^6 \right] \quad (5)$$

$$V_{\text{cm}}(\mathbf{R}) = \sum_{j=x,y,z} V_j \left[2k_j^2 R_j^2 - \frac{2}{3} k_j^4 R_j^4 + \frac{4}{45} k_j^6 R_j^6 \right] \quad (6)$$

$$W(\mathbf{r}, \mathbf{R}) = \sum_{j=x,y,z} V_j \left[-k_j^4 r_j^2 R_j^2 + \frac{1}{3} k_j^6 r_j^2 R_j^4 + \frac{1}{12} k_j^6 r_j^4 R_j^2 \right], \quad (7)$$

respectively, shows that the quartic terms all have a negative sign which makes the expansion to the sextic degree necessary. Otherwise, an unphysical continuum would occur in the spectrum reaching in energy towards negative infinity. In Eqs. (5)-(7) V_j is the lattice depth in direction $j \in \{x, y, z\}$, $k_j = \frac{2\pi}{\lambda_j}$, and λ_j is the wavelength of the laser in direction j . Introducing the harmonic oscillator frequencies $\omega_j^2 = \frac{2V_j}{m} k_j^2$ the potential terms can be written in a more canonical form.

It has been demonstrated [4, 5, 12] that sextic potentials are well suited to describe anharmonicity-induced c.m.-rel. coupling in single-well potentials. The large flexibility in the potential parameters makes the sextic potential, moreover, suitable to accurately describe the c.m.-rel. coupling in a variety of potentials, e. g. Gaussian beam potentials [12].

It is first assumed that the anharmonicity only has a small (global) influence on the eigenenergies of the states. Hence, the harmonic approximation is used and the position of a c.m.-rel. coupling resonance is determined by the position of the crossing of the c.m. excited bound state $|\psi_b \Phi_{\mathbf{n}}\rangle$, where $\mathbf{n} = (n_x, n_y, n_z)$ is the quantum number of the c.m. excitation, that separates spatially for an optical-lattice potential, and a trap state $|\psi_t \Phi_{\mathbf{m}}\rangle$ as illustrated in Fig. 1.

The energy E_b^{rel} of the bound state $|\psi_b\rangle$ in an harmonic confinement of arbitrary anisotropy in dependence of the s -wave scattering length a is given implicitly by [27]

$$\frac{\sqrt{\pi} d_y}{a} = - \int_0^\infty \left(\frac{\sqrt{\eta_x \eta_z} e^{\frac{\epsilon}{2}}}{\sqrt{(1-e^{-t})(1-e^{-\eta_x t})(1-e^{-\eta_z t})}} - t^{-\frac{3}{2}} \right) dt \quad (8)$$

where $\epsilon = (E_b^{\text{rel}} - E_0)/(\hbar\omega_y)$, $E_0 = \frac{\hbar}{2}(\omega_x + \omega_y + \omega_z)$, $\eta_x = \omega_x/\omega_y$, and $\eta_z = \omega_z/\omega_y$. The difference to other equations for the bound state, like e.g. in [1] (valid for a 3D isotropic confinement), in [23] (valid for a 3D harmonic confinement of single anisotropy), or in [28] (valid for only transversally trapped atoms), is that it is valid for an arbitrarily anisotropic 3D confinement.

A general expression for the eigenenergies of the trap states in an arbitrarily anisotropic confinement, i.e. states above $E_{\text{th}} = \frac{\hbar}{2}(\omega_x + \omega_y + \omega_z)$, is not known yet. For ultracold temperatures the occupation of excited states is suppressed. Hence, in the following only crossings with the first trap state $|\psi_1\rangle$ are considered. Assuming without loss of generality that $\min(\omega_x, \omega_y, \omega_z) = \omega_z$ (unless stated differently), the eigenenergy E_1^{rel} of $|\psi_1\rangle$ lies in the interval $[E_{\text{th}}, E_{\text{th}} + 2\hbar\omega_z)$. It can be shown that in the case of an isotropic harmonic confinement the crossing between an excited bound state with a single lowest-order c.m. excitation ($n_i = 2, n_{j \neq i} = 0$) with the first trap state occurs at

$$E_1^{\text{rel}} = E_{\text{th}} + \hbar\omega_z \quad (9)$$

which is thus chosen for the model as an approximation of the energy of the first trap state. For crossings with higher trap states, the model can be extended by the proper choice of the energy of that trap state.

For a spatially decoupled confinement, like expansions of an optical-lattice potential, the eigenstates of the c.m. Hamiltonian factorize as $\Phi_{\mathbf{n}}(\mathbf{R}) = \phi_{n_x}(X) \phi_{n_y}(Y) \phi_{n_z}(Z)$ with eigenenergies $E_{\mathbf{n}}^{\text{cm}} = \sum_{j=x,y,z} \hbar\omega_j(n_j + \frac{1}{2})$. When combining rel. and c.m. motions the energies of the bound states become $E_b^{\text{rel}}(a) + E_{\mathbf{n}}^{\text{cm}}$ while the energy of the lowest trap state is given by $E_1^{\text{rel}} + E_{(0,0,0)}^{\text{cm}}$. Crossings between a c.m. excited bound state and the lowest trap state are determined by

$$E_b^{\text{rel}} = E_1^{\text{rel}} - \Delta_{\mathbf{n}} \quad (10)$$

where

$$\Delta_{\mathbf{n}} = E_{\mathbf{n}}^{\text{cm}} - E_{(0,0,0)}^{\text{cm}} \quad (11)$$

is the c.m. excitation. The corresponding s -wave scattering length at the crossing is obtained from Eq. (8).

So far all energies were treated within the harmonic approximation. It will be demonstrated that this purely harmonic model gives in some cases already good quantitative results. However, for the c.m. excitations $\Delta_{\mathbf{n}}$ higher c.m. states are involved. Additionally, for small $\Delta_{\mathbf{n}}$ the bound state crosses the trap state for small positive d_{ho}/a or even negative d_{ho}/a where the two states cross with comparable slopes, see Fig. 1. For such crossings the position is very sensitive to the energies of the involved states. Hence, the energy of the first trap state as well as the c.m. excitation Δ must be corrected.

Treating the anharmonic terms of the c.m. potential in Eq. (6), $\sum_{j=x,y,z} -\frac{1}{24} \frac{\hbar\omega_j}{V_j} R_j^4 + \frac{1}{720} \frac{\hbar^2\omega_j^2}{V_j^2} R_j^6$ (here written in dimensionless units of energies in $\hbar\omega_j$ and lengths in $\sqrt{\frac{\hbar}{M\omega_j}}$ with $M = 2m$) within first-order perturbation theory results in

$$\Delta_{(n_x, n_y, n_z)} = \sum_{j=x,y,z} \hbar\omega_j \left[n_j - \frac{\hbar\omega_j}{16V_j} (n_j^2 + n_j) + \frac{\hbar^2\omega_j^2}{576V_j^2} (2n_j^3 + 3n_j^2 + 4n_j) \right] \quad (12)$$

for the c.m. excitation and

$$E_1^{\text{rel}} = \hbar\omega_z + \sum_{j=x,y,z} \frac{1}{2} \hbar\omega_j - \frac{\hbar\omega_j^2}{32V_j} + \frac{\hbar\omega_j^3}{384V_j^2} \quad (13)$$

for the energy of the first trap state (see Section XB in the Appendix for details).

It will be demonstrated that in the case of resonances for negative values of the s -wave scattering length and strongly anisotropic confinement, the effective 1D c.m. problem needs even to be solved exactly and thus numerically to obtain accurate results. For the numerical evaluation of the stationary 1D Schrödinger equation, the approach described in [29] was used.

Therefore, three models for the resonance position were introduced that differ by the treatment of the c.m. excitation Δ and by the energy of the first trap state E_1^{rel} . In *model A*, Δ and E_1^{rel} are given in the harmonic approximation by Eqs. (11) and (9), in *model B* by Eqs. (12) and (13) within a perturbative correction, respectively, and in *model C* the c.m. energies are calculated numerically exact. For given Δ and E_1^{rel} within one model, the inelastic CIR position for a c.m. excitation is then determined by Eq. (10).

IV. C.M.-REL. COUPLING MODEL – COUPLING STRENGTHS

After having introduced a straightforward procedure to evaluate the resonance positions using a model (with three different versions A, B, and C) for the resonance positions, the coupling strengths are considered. They are of particular interest for experiments, since they determine the width and thus experimental visibility. Furthermore, they are, e. g., necessary for a Landau-Zener treatment of the dynamics at the resonances that allows for an estimate whether diabatic or adiabatic transitions between the involved states occur at the avoided level crossings. The matrix element defining the coupling strength $W_{\mathbf{n}}$ between a bound state $|\psi^{(b)}(\mathbf{r}) \Phi_{\mathbf{n}}(\mathbf{R})\rangle$ with c.m. excitation $\Delta_{\mathbf{n}}$ and the lowest trap state $|\psi_1(\mathbf{r}) \Phi_{(0,0,0)}(\mathbf{R})\rangle$ is

$$W_{\mathbf{n}} = \langle \psi^{(b)}(\mathbf{r}) \Phi_{\mathbf{n}}(\mathbf{R}) | W(\mathbf{r}, \mathbf{R}) | \psi_1(\mathbf{r}) \Phi_{(0,0,0)}(\mathbf{R}) \rangle. \quad (14)$$

For the model the wavefunctions of a harmonic confinement are adopted. Hence, the c.m. wavefunction is the product of 1D harmonic oscillator wavefunctions (here written in dimensionless units of energies in $\hbar\omega_j$ and lengths in $\sqrt{\frac{\hbar}{M\omega_j}}$)

$$\Phi_n(R_j) = \pi^{-\frac{1}{4}} \sqrt{\frac{1}{2^n n!}} e^{-\frac{1}{2}R_j^2} H_n(R_j) \quad (15)$$

where $H_n(R_j)$ denote the Hermite polynomials. The c.m. integral in Eq. (14) reduces to a sum of 1D integrals that can be calculated even analytically.

The 3D integral over the relative-motion coordinate is more laborious. While an expression for the trap wavefunctions for an arbitrarily anisotropic harmonic confinement is so far (to the authors' knowledge) not yet known, a general solution for the trap state in a harmonic potential with a single (but arbitrary) anisotropy, e. g. $\omega_x = \omega_y =: \omega_{\perp} \neq \omega_z$ is given in [23]. However, the numerical evaluation of Eq. (14) with the most general version of the relative motion wavefunction given in [23],

$$\begin{aligned} \psi_{\epsilon}(\rho, z) &= \frac{\eta}{2\pi^{3/2} 2^{\epsilon/2}} e^{-\eta\rho^2/2} \\ &\times \sum_{m=0}^{\infty} 2^{m\eta} L_m(\eta\rho^2) \Gamma\left(\frac{2m\eta - \epsilon}{2}\right) D_{\epsilon-2m\eta}(\sqrt{2}|z|), \end{aligned} \quad (16)$$

has turned out prohibitively demanding. In the regime of a strongly elongated (quasi-1D) potential the expression greatly simplifies [23] to

$$\psi_1(\rho, z) = \frac{\eta}{2\pi^{3/2} 2^{\epsilon/2}} e^{-\eta\rho^2/2} \Gamma\left(-\frac{\epsilon}{2}\right) D_{\epsilon}\left(\sqrt{2}|z|\right). \quad (17)$$

In these equations D_{ν} denotes the parabolic cylinder function, L_m the Laguerre polynomials, Γ the gamma

function, and $\rho^2 = x^2 + y^2$. The wavefunctions are written in dimensionless units of energies in $\hbar\omega_z$ and lengths in $d_z = \sqrt{\frac{2\hbar}{m\omega_z}}$. Moreover, the previously introduced definitions $\eta = \frac{\omega_{\perp}}{\omega_z}$ and $\epsilon = E^{\text{rel}} - \frac{\hbar}{2}(\omega_x + \omega_y + \omega_z)$ remain valid. Within the model (see above), the energy at the resonance is $\epsilon = \hbar\omega_z$ (assuming that the elongation of the trap is along the z direction). It is important that for the wavefunction the energy is *not* corrected by the anharmonic terms, because this might result in a different energy branch of the spectrum. With $\epsilon = \hbar\omega_z$ at the resonance, Eq. (17) can be further simplified (in physical units) to

$$\psi(\rho, z) = \frac{\sqrt{2}\Gamma\left(-\frac{1}{2}\right)}{4\pi^{\frac{3}{2}} d_{\perp}^2 \sqrt{d_z}} |z| \exp\left(-\frac{\rho^2}{2d_{\perp}^2} - \frac{z^2}{2d_z^2}\right) \quad (18)$$

with $d_{\perp} = \sqrt{\frac{2\hbar}{m\omega_{\perp}}}$ and using that for integer n the relation $D_n(x) = 2^{-\frac{n}{2}} e^{-\frac{x^2}{4}} H_n\left(\frac{x}{\sqrt{2}}\right)$ holds.

In quasi 2D, the wavefunction can be simplified to [23]

$$\psi_1(\rho, z) = \frac{1}{2\pi^{\frac{3}{2}}} e^{-\frac{\eta\rho^2 + z^2}{2}} \Gamma\left(-\frac{\epsilon}{2\eta}\right) U\left(-\frac{\epsilon}{2\eta}, 1, \eta\rho^2\right) \quad (19)$$

where U denotes the confluent hypergeometric function. Again, dimensionless units of energy in $\hbar\omega_z$ and lengths in d_z are used.

The rel. motion bound-state wavefunction [23]

$$\begin{aligned} \psi_b(\mathbf{r}) &= \frac{\sqrt{d_z}}{d_{\perp}^2 (2\pi)^{3/2}} \\ &\times \int_0^{\infty} dt \frac{\exp\left(t\frac{E}{\hbar\omega_z} - \frac{z^2}{2td_z^2} - \frac{\rho^2}{2d_{\perp}^2} \coth\left(\frac{td_z^2}{d_{\perp}^2}\right)\right)}{\sqrt{t} \sinh\left(\frac{td_z^2}{d_{\perp}^2}\right)}. \end{aligned} \quad (20)$$

which is written here in physical units, is valid for an isotropic confinement as well as for a strongly anisotropic trap geometry. Note, if the energy of the bound state crosses the energy of the trap state for positive values of the s -wave scattering length that are sufficiently small ($a \lesssim d_{\perp}$), its energy at the crossing is sufficiently small such that the bound state wavefunction can be described in good approximation by its trap-free counterpart

$$\psi_{\text{free}}(r) = \frac{1}{\sqrt{2\pi a}} \frac{e^{-\frac{r}{a}}}{r}. \quad (21)$$

However, for crossings at negative s -wave scattering lengths, this approximation certainly fails, because in the free case the bound state only exists for $a > 0$. Hence, in the following Eq. (20) is used for the bound-state wavefunction.

The wavefunctions of a harmonic confinement of *simple* anisotropy are used for the model. Therefore, the

rel. motion integral is reduced to a two-dimensional one where the coupling term $W(\mathbf{r}, \mathbf{R})$ is averaged over the transversal direction, $\omega_{\perp} = \frac{1}{2}(\omega_x + \omega_y)$. The matrix element becomes

$$W_{\mathbf{n}} = 2\pi \int_0^{\infty} d\rho \rho \int_{-\infty}^{\infty} dz \psi_b(\rho, z) \psi_1(\rho, z) \tilde{W}(\rho, z) \quad (22)$$

with

$$\begin{aligned} \tilde{W}(\rho, z) = & \sum_{k=x,y} V_k \int_{-\infty}^{\infty} dR_k W_k(\rho, R_k) \Phi_{n_k} \Phi_{n_0} \\ & + V_z \int_{-\infty}^{\infty} dZ W_z(z, Z) \Phi_{n_z} \Phi_{n_0} \end{aligned} \quad (23)$$

where $W(\mathbf{r}, \mathbf{R}) = \sum_{j=x,y,z} V_j W_j(r_j, R_j)$ and $\mathbf{n} = (n_x, n_y, n_z)$.

Hence, different to the resonance position where three models were introduced that differed in the treatment of the c.m. energies, two models for the coupling strength were introduced that differ in the way the rel.-motion wavefunction ψ_1 is treated. In quasi 1D, Eq. (18) is used for ψ_1 within *model 1*, in quasi 2D Eq. (19) is adopted for ψ_1 within *model 2*. The models solve the coupling matrix element of Eq. (14) for the exact coupling term of the sextic potential of Eq. (7) with wavefunctions in the harmonic approximation.

V. 3D-1D TRANSITION

In order to characterize the behavior of the resonances and to validate the models, full six-dimensional *ab initio* calculations are performed. The numerical algorithm to solve the stationary Schrödinger equation for the Hamiltonian in Eq. (1) is described in [24]. For the efficient computational treatment of ultracold atoms in optical lattices the basis functions are symmetry adapted to the eight irreducible representations ($A_g, B_{1g}, B_{2g}, B_{3g}, A_u, B_{1u}, B_{2u}, B_{3u}$) of the orthorhombic point group D_{2h} . This leads to a corresponding block structure of the Hamiltonian matrix. As a realistic example for an interatomic interaction potential U_{int} the (numerically given) Born-Oppenheimer potential curve of two ${}^7\text{Li}$ atoms in the electronic state $a^3\Sigma_u^+$ are used in this work, see [17] for details on how this potential was obtained. The variation of the s -wave scattering length is achieved by slight modifications of the inner-wall of the potential [30] which effectively changes the asymptotic behavior of the radial wavefunction and hence the s -wave scattering length. Resonance positions and coupling strengths are extracted from the *ab initio* data by fitting a two-channel model to the corresponding avoided energy crossing (see Section X A in the Appendix).

In the following, the behavior of the coupling resonances is investigated in the transition from a 3D to a quasi-1D confinement. Two ${}^7\text{Li}$ atoms are considered in a sextic potential (Eqs. (5)-(7)) with $\lambda=1000$ nm,

$\omega_x/\omega_y = 1.1$, $V_y = 35.9 E_r$. To obtain an elongation in the longitudinal z direction, the potential depth V_z is decreased. Hence, an almost spherical potential is deformed into an elongated, cigar-shaped one.

The coupling term W in Eq. (7) is totally symmetric and hence only states of equal symmetry couple. Since in the following only crossings with the first trap state without a c.m. excitation are considered, only even excitations, i. e. states with even n_j , can couple. Moreover, in the *ab initio* calculation it suffices to consider the A_g symmetry because the states involved in the considered inelastic CIR, the first trap state, the last bound state and the even c.m. excitations possess A_g symmetry, see [24] for details.

The two lowest-order transversal resonances with (2, 0, 0) and (0, 2, 0) c.m. excitation and the first-order longitudinal resonance with (0, 0, 4) c.m. excitation are investigated in the following. These resonances are selected because they are the most pronounced ones. As a rule of thumb, the coupling between a c.m. excited bound state and the ground trap state decreases with the order of the c.m. excitation, i. e. the lowest resonances $n_i = 2, n_{j \neq i} = 0$ show the strongest coupling. A simple argument for this rule is that the stronger oscillations in higher excited c.m. bound states decrease the overlap to the trap state and hence also the coupling matrix element Eq. (14). Numerically, this rule is veri-

\mathbf{n}	(0, 2, 0)	(0, 2, 2)	(0, 4, 0)	(0, 6, 0)	(0, 8, 0)
$W_{\mathbf{n}} [10^{-3} \hbar \omega_y]$	3.19	1.46	0.795	0.50	0.31

Table I. Coupling strengths $W_{\mathbf{n}}$ for $\omega_x/\omega_y = 1.1$, $\omega_y/\omega_z = 1$, $V_y = 35.9 E_r$ of the first trap state with c.m. excited bound states for different c.m. excitations \mathbf{n} obtained with the model 1.

fied by calculating the coupling matrix element Eq. (14) for different c.m. excitations, see Table I, confirming that $W_{\mathbf{n}}$ decreases with an increasing order of the c.m. excitation. It can also be seen in the energy spectrum in Fig. 2 where high-order resonances do not show visible avoided crossings [31]. The fact that the coupling decreases with the c.m. excitation of the bound state delivers an explanation why in [15] it is (correctly) concluded that the dimer-production rate at an c.m.-rel. coupling resonance involving a very highly c.m.-excited bound state is negligible.

While lowest-order resonances show the strongest coupling, in the following the lowest-order longitudinal resonance with c.m. excitation (0, 0, 2) is not considered because its position fades away to $\frac{d_y}{a} \ll -1$ with decreasing ω_z where the bound state is very shallow and has lost its characteristic small interatomic distance. In the full spectrum the crossing can therefore not be easily resolved any more. This can be seen in Fig. 2 in the upper most panel, where the energy of the $|\psi_b \Phi_{(0,0,2)}\rangle$ state asymptotically approaches $|\psi_1 \Phi_{(0,0,0)}\rangle$ without a pronounced crossing.

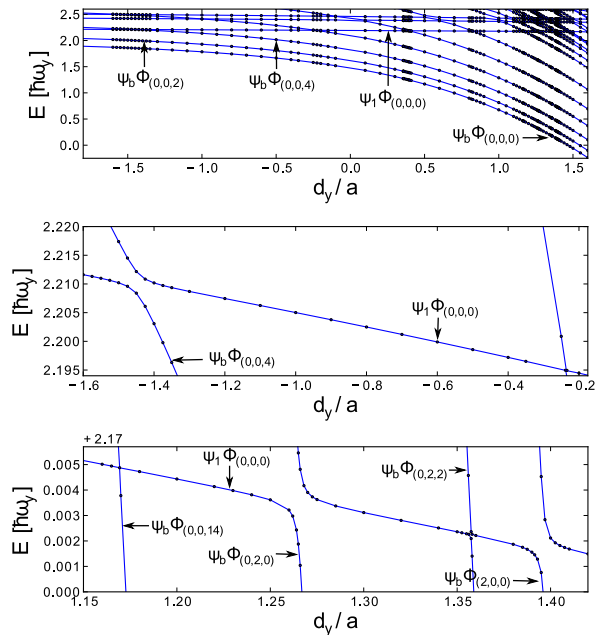


Figure 2. (Color online) *Ab initio* energy spectrum of a ${}^7\text{Li}-{}^7\text{Li}$ system confined in a sextic trapping potential with $\lambda=1000$ nm, $\omega_x/\omega_y = 1.1$, $\omega_y/\omega_z = 10$, $V_y = 35.9 E_r$. The labels of the energy branches denote the corresponding diabatic states.

In Fig. 3 the three considered resonance positions of the models with different degrees of corrections together with *ab initio* results are shown. Before discussing the validity of the models, the behavior of the resonances is analyzed. For small anisotropies $\omega_y/\omega_z \lesssim 2$ the $(0,0,4)$ resonance lies at larger values of d_y/a (the green curve lies above the red and blue curves in Fig. 3) simply because the c.m. excitation $\Delta_{(0,0,4)}$ is larger than $\Delta_{(0,2,0)}$ and $\Delta_{(2,0,0)}$. Therefore, the c.m. excited bound state $|\psi_b \Phi_{(0,0,4)}\rangle$ crosses at larger values of d_y/a than the ones with a single excitation. A decrease of $V_z \propto \omega_z^2$ decreases the spacings of the states that have a c.m. excitation in the z direction. Hence, for decreasing ω_z the $(0,0,4)$ resonance crosses constantly at smaller values of d_y/a which explains the monotonic decrease of the *ab initio* results in Fig. 3 (green squares). On the other hand, the transversal c.m. excitations ($\Delta_{(0,2,0)}$ and $\Delta_{(2,0,0)}$) remain constant for a variation of ω_z . Yet, a decrease in ω_z also decreases the energy of the first trap state. Therefore, the transversally excited c.m. states $|\psi_b \Phi_{(2,0,0)}\rangle$ and $|\psi_b \Phi_{(0,2,0)}\rangle$ cross at larger values of d_y/a with decreasing ω_z converging to a finite value as $\omega_z \rightarrow 0$.

Next, the validity of the models is considered. For the transversal $(2,0,0)$ and $(0,2,0)$ resonances the perturbative corrections Eqs. (12) and (13) agree with the numerically exact corrections (the dashed and solid lines are indistinguishable). The resonance positions resulting from the harmonic approximation (dashed-dotted lines, model A) show an almost constant offset towards larger values compared to model B were the anharmonicity in

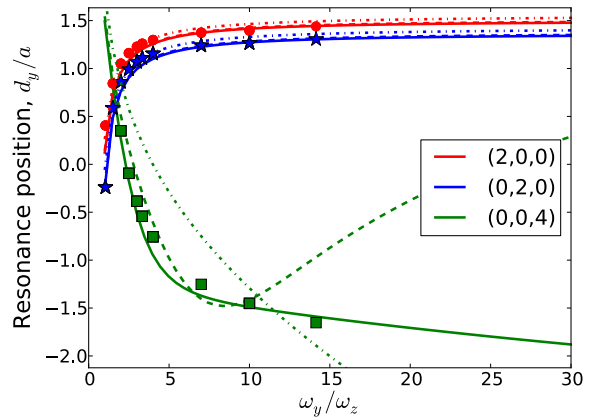


Figure 3. (Color online) Resonance positions for different c.m. excitations $\mathbf{n} = (n_x, n_y, n_z)$ (see legend) obtained by full *ab initio* calculations [dots $(2,0,0)$, stars $(0,2,0)$, squares $(0,0,4)$] and the model (lines) if the tightness in z direction is reduced. The dashed-dotted lines correspond to the harmonic approximation (model A). The dashed lines are obtained by a perturbative correction of the energies (model B). For the solid lines, the correction is calculated in a numerically exact way (model C).

the c.m. motion has been taken into account. This small offset is due to the missing negative quartic term that is present for the sextic potential. Certainly, the models give very good quantitative agreement with the *ab initio* calculations. For strong anisotropies the results of the models B and C (dashed and solid lines) are in perfect quantitative agreement, e. g., at $\omega_y/\omega_z = 10$ the models give $d_y/a = 1.397$ and the *ab initio* method results in $d_y/a = 1.396$ for the $(2,0,0)$ resonance. This excellent applicability of the model for the resonance positions in the quasi-1D regime lead to the quantitative agreement of the model compared to the loss resonances measured in [7] as shown in [5].

The results for the longitudinal $(0,0,4)$ resonances are more sensitive. First, with a decreasing potential depth the anharmonicity is important already for low lying states. Second, for the $(0,0,4)$ resonance higher c.m. excitations are involved which enhances the influence of the anharmonicity. Moreover, for a decreasing resonance position the bound state crosses the trap state with an increasingly comparable slope which makes the position more sensitive to energy variations. Therefore, model A including uncorrected, harmonic c.m. excitation is inaccurate over the entire range of anisotropies. The perturbatively corrected model B is acceptable for mild anisotropies ($\omega_y/\omega_z \lesssim 10$) but has a wrong behavior for $\omega_y/\omega_z \gtrsim 10$. Finally, model C which corrects the c.m. excitations and the energy of the trap state exactly numerically is quantitatively accurate over the entire range of the scattering length, even in the limit $\omega_z \rightarrow 0$ (green solid line).

The quantitative accuracy for very large values of the

anisotropy, $\omega_y/\omega_z \gtrsim 10$, could not be confirmed by the *ab initio* method [24]. The basis set of the method consists of spherical harmonics which are not well suited for resolving extremely anisotropic wavefunctions unless high angular-momentum quantum numbers are employed which leads to an inconvenient scaling of the numerical effort.

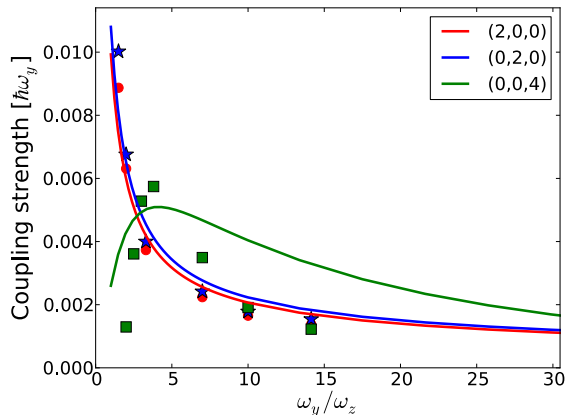


Figure 4. (Color online) Coupling strength for different c.m. excitations $\mathbf{n} = (n_x, n_y, n_z)$ (see legend) obtained by full *ab initio* calculations [dots (2,0,0), stars (0,2,0), squares (0,0,4)] and the model 1 (solid lines).

In Fig. 4 the coupling strengths corresponding to Fig. 3 are shown. Again, the overall behavior is discussed prior to the validity of the model 1. The coupling strength of the transversal resonances with (2,0,0) and (0,2,0) c.m. excitations (red circles and blue stars, respectively) decreases monotonically with increasing anisotropy but approaches a constant value for $\omega_z \rightarrow \infty$. Otherwise the observation of the (2,0,0) and (0,2,0) resonances in [7] where the anisotropy of the external confinement is $\approx 10^3$ would not have been possible. A simple argument for the monotonic decrease is that $W(\mathbf{r}, \mathbf{R}) \propto V_k$.

For the resonance with longitudinal (0,4,0) c.m. excitation, a non-monotonic behavior is visible. In the limit of $\omega_z \rightarrow 0$ which corresponds to a zero potential in the z direction, the coupling of the resonances with a c.m. excitation in the longitudinal direction vanishes. This is intuitive, since without a confinement potential there exists no confinement-induced c.m.-rel. coupling. On the other hand, a decrease in the potential depth V_z leads to an enhancement of the anharmonicity-induced coupling, since the potential becomes more anharmonic (this will be discussed in more detail in Section VII). The result of these counter-acting effects is the non-monotonic curve with the local maximum for the (0,0,4) resonance and a vanishing coupling for $\omega_z \rightarrow 0$.

Next, the validity of model 1 is considered. For the longitudinal resonance, model 1 provides the correct qualitative behavior and reproduces the local maximum accurate in position. In general, however, it does not provide highly accurate quantitative agreement. Especially

for larger anisotropies ($\omega_y/\omega_z \gtrsim 7$), the model 1 overestimates the coupling strengths. Again, this behavior is understandable since for the higher-order longitudinal resonances the anharmonicity becomes increasingly important, which cannot be modeled accurately with wavefunctions in the harmonic approximation.

For the transversal resonances with $\Delta_{(0,2,0)}$ and $\Delta_{(2,0,0)}$ c.m. excitation, the coupling strengths predicted by the model 1 agree quantitatively very well with the *ab initio* ones for $\omega_y/\omega_z \geq 2$. This agreement is remarkable, since no free parameters were used in the models.

VI. 3D-2D TRANSITION

In the following, the transition from a 3D to a quasi-2D confinement is considered. Again, as a realistic example two ^7Li atoms in a sextic confinement of $\lambda=1000$ nm and $V_y=35.9E_r$ are chosen. To obtain a pancake-shaped trap ω_x and ω_z are decreased, keeping the ratio $\omega_x/\omega_z = 1.1$ constant. The lowest-order resonance with (0,2,0) c.m. excitation and the next to leading order resonances with $\mathbf{n} = (4,0,0)$ and $\mathbf{n} = (0,0,4)$ are considered. Again, in analogy to the 1D case these resonances are the most pronounced ones, having in mind that the two lowest-order resonances with excitations in the weakly confined directions, i. e. with c.m. excitations (2,0,0) and (0,0,2), fade away towards large negative values of d_y/a , loosing their resonant character.

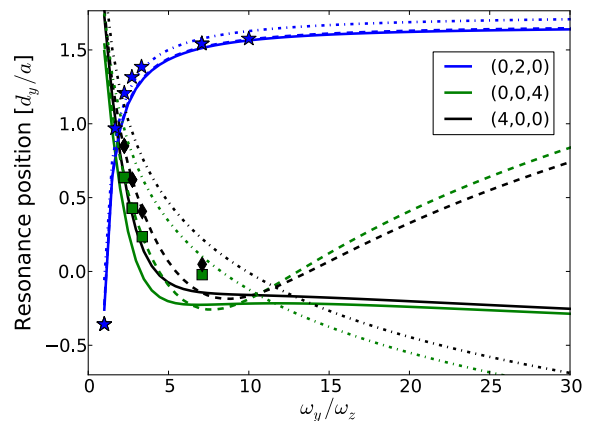


Figure 5. (Color online) Resonance positions for different c.m. excitations obtained by full *ab initio* calculations (dots) and the model (lines). The dashed lines are obtained by the perturbative correction of the energies (model B), the solid lines indicate the numerically exact c.m. correction (model C) and the dashed-dotted lines correspond the harmonic approximation (model A).

As before, the behavior of the resonance positions in Fig. 5 is discussed first based on the *ab initio* results. A similar behavior as for the 1D case is visible. By the same arguments that hold in the 3D to 1D transition, the (0,2,0) resonance with excitation in the strongly

confined direction starts at negative values of d_y/a for small anisotropies and converges to an asymptotic value for strong anisotropies ($\omega_x, \omega_z \rightarrow 0$). The higher order (4, 0, 0) and (0, 0, 4) resonances start at positive values of d_y/a at small anisotropies and do not converge to an asymptotic value for $\omega_x, \omega_z \rightarrow 0$.

For the (0, 2, 0) resonance, the model A is again shifted to slightly higher resonance positions due to the absence of a negative quartic term. While for intermediate anisotropies the harmonic theory gives slightly better quantitative agreement to the *ab initio* calculations, the asymptotic value is quantitatively reproduced to high accuracy within the corrected model B, where a perturbative treatment of the energy corrections is sufficient.

For the higher order (4, 0, 0) and (0, 0, 4) resonances, the perturbative treatment of the corrections gives an almost perfect quantitative description of the resonance positions for mild anisotropies. However, for strong anisotropies it fails (shows a minimum in the resonance positions and then goes to positive values of d_y/a) and the exact treatment of the 1D c.m. excitation within model C delivers the most accurate results.

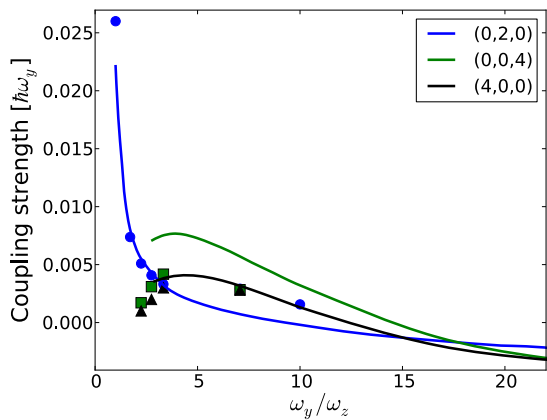


Figure 6. (Color online) Coupling strength for different c.m. excitations $\mathbf{n} = (n_x, n_y, n_z)$ (see legend) obtained by full *ab initio* calculations [dots (0,2,0), squares (0,0,4), triangles (4,0,0)] and the model 2 (solid lines).

In Fig. 6 the coupling strengths for the transition from a 3D to a quasi-2D confinement are shown. The *ab initio* results show a constant decrease for the (0, 2, 0) resonance. This is in analogy to the resonances with excitations in the strongly confined direction in the transition to a cigar-shaped potential shown in Fig. 4. Again, the decrease can be explained by the decrease of the coupling potential $W(\mathbf{r}, \mathbf{R}) \propto V_k$ if V_x and V_z are reduced in the transition to a pancake-shaped confinement.

The behavior of the coupling strengths of the (4, 0, 0) and (0, 0, 4) resonances in a pancake-shaped confinement exhibits a similar behavior as the longitudinal (0, 0, 4) resonance in a cigar-shaped confinement shown in Fig. 4. The *ab initio* results demonstrate that the coupling strength is close to zero for an almost isotropic confine-

ment (that is why it cannot be resolved for $\omega_y/\omega_z \lesssim 2$), increases until it reaches a maximum and then falls off to zero as $\omega_x, \omega_z \rightarrow 0$. Again, its behavior is a result of the counter-acting effect that on one hand decreasing the potential depth increases the anharmonicity and hence the coupling strength, but on the other hand $\omega_z \rightarrow 0$ corresponds to switching off the confinement leading to a vanishing confinement-induced coupling.

A breakdown of model 2 is detected for very large anisotropies ($\omega_y/\omega_z > 10$) where the model 2 predicts negative coupling strengths for all resonances. The reason why the coupling integral in Eq. (22) can result in negative values is the negative quartic term in Eq. (7). However, while negative coupling strengths for themselves are not a problem yet, an unphysical discontinuity is introduced when taking the absolute value. Hence, the sign change (or even vanishing value) of the coupling strength is unphysical. Since such a behavior is absent for the cigar-shaped regime, the used harmonic quasi-2D trap state wavefunction, Eq. (19) turns out to be inappropriate here.

Still, the model 2 reproduces correctly the decreasing coupling strength for the (0, 2, 0) resonance. For smaller anisotropies $\omega_y/\omega_z \lesssim 5$ it is even quantitatively accurate. For the (4, 0, 0) and (0, 0, 4) resonances, the non-monotonic behavior is reproduced qualitatively.

In general, for the positions as well as for the coupling strengths, the models in quasi 1D show a better quantitative agreement than the corresponding models in quasi 2D, simply because for a single decreasing potential depth the anharmonicity effects are milder compared to the pancake-shaped potential and can be reproduced by the model that is based on the harmonic approximation more accurately.

VII. SIMULTANEOUS VARIATION OF THE POTENTIAL DEPTH

It is an important question how the c.m.-rel. coupling can be optimized. As demonstrated above, the coupling at the lowest-order resonances, i. e. with c.m. excitations $n_i = 2, n_{j \neq i} = 0$, and with excitations in the tightly confined direction have a peak coupling strength for an isotropic trap and then monotonically decrease with the anisotropy, i. e. with a decreasing potential depth in the weakly confined direction(s).

Higher-order resonances in the weakly confined direction(s) have a very small coupling for an isotropic confinement, peak at mild anisotropies and then decrease to zero for increasing anisotropies.

In general, the coupling strength can also be modified by a simultaneous variation of the potential depth, i. e. by a variation of all potential depths and not only selected ones leading to a different (quasi-1D or quasi-2D) trap geometry. The *ab initio* results in Table II demonstrate that the coupling increases with a decrease of the potential depth V . This behavior can be understood in-

V_y/E_r	53.9	36.0	18.0	9.0	4.5
$W_{\text{ab initio}}[10^{-3}\hbar\omega_y]$	7.7	9.3	13.2	19.0	25.0
$W_{\text{model}}[10^{-3}\hbar\omega_y]$	5.2	5.9	6.7	6.3	2.6

Table II. Coupling strengths $W_{\mathbf{n}}$ for $\omega_x/\omega_y = 1$, $\omega_y/\omega_z = 0.5$ of the $(0, 2, 0)$ resonance for different values of the potential depth for *ab initio* calculation and model 1.

tuitively. As the potential becomes deeper, the harmonic approximation becomes more accurate and it has a zero c.m.-rel. coupling. While the model follows this behavior for a deep potential, it loses the accuracy, if the potential gets to shallow, and results in an unphysical decrease of the coupling. The reason for this failure of the model is that the harmonic wavefunctions become less accurate for a decreasing potential depth.

In the case of an optical lattice, the decrease of the potential depth has yet another important consequence. A tunnel coupling between neighboring wells enhances drastically the c.m.-rel. coupling. In fact, *ab initio* calculations of a double and a quadruple-well potential have shown that in this case even high-order resonances show a considerable coupling. Moreover, the results of the calculation explain some of recently measured loss resonances in a shallow 3D optical lattice in an ultracold gas of Cs atoms [32].

V_y/E_r	53.9	36.0	18.0	9.0	4.5
$d_y/a_{\text{ab initio}}$	0.9	0.91	0.92	0.9	0.81
d_y/a_{model}	0.82	0.8	0.77	0.72	0.66

Table III. Resonance position for $\omega_x/\omega_y = 1$, $\omega_y/\omega_z = 2$ of the $(0, 2, 0)$ resonance for different values of the potential depth for *ab initio* calculations and the model B with the perturbative energy correction. The harmonic approximation of the model A predicts a resonance position of $d_y/a = 0.886$ independent of V .

With a decreasing potential depth the harmonic approximation of the potential becomes inaccurate and the limitations of the introduced models become visible. In Fig. 3 a good agreement of the harmonic approximation was visible for the positions, especially for small anisotropies. In the harmonic approximation, i. e. without the energy corrections in Eqs. (12) and (13), the position of the resonances is independent of the potential depth. However, with decreasing potential depth, the anharmonic terms in the sextic potential start to have a significant influence already at energies of the lowest trap state and hence influence the resonance positions. In Table III the dependence of the position for a mild anisotropy is compared for the model B and *ab initio* calculations. While the *ab initio* results are almost constant for a deep potential, the resonance position decreases for a decreasing potential depth to small values. While the model A in the harmonic approximation is independent

of the potential depth, the energy-corrected model B reflects this decrease reasonably.

VIII. WAVEFUNCTION ANALYSIS

C.m.-rel. coupling resonances have been directly observed experimentally in a two-body system via coherent molecule formation [12] and indirectly in a many-body system in terms of particle loss and heating [5, 7]. The latter is a consequence of the molecule formation at the resonance. Both measurements detected resonances where the bound state was excited in a strongly confined direction, i. e. in quasi-1D the $(2, 0, 0)$ and $(0, 2, 0)$ resonances [7, 12], and in quasi-2D the $(0, 2, 0)$ resonance [7] was detected. Due to the anisotropy of the confinements, the resonance position occurred for positive values of the s -wave scattering length. It was demonstrated above, see, e. g. Fig. 3, that also resonances at negative values of the s -wave scattering length occur: for lowest-order resonances if the anisotropy is kept small, or for higher-order resonances for a stronger anisotropy of the confinement.

In the following, *ab initio* wavefunctions are analyzed for the system of two ${}^7\text{Li}$ atoms confined to a sextic potential with parameters $\lambda=1000$ nm, $\omega_x/\omega_y = 1.1$, $\omega_x/\omega_z = 10$, $V_y = 35.9 E_r$. The corresponding energy spectrum is shown in Fig. 2. Considered are the densities of the bound and trap states involved in the transversally excited $(2, 0, 0)$ resonance and the longitudinally excited $(0, 0, 4)$ resonance. The positions at which the wavefunctions are investigated are chosen such that the overlaps of the involved trap and the bound states are still small in order to compare the characteristics of the states. This is $d_y/a = 1.42$ for the $(2, 0, 0)$ and $d_y/a = -1.2$ for the $(0, 0, 4)$ resonance, respectively.

In Fig. 7 cuts through the trap-state densities are shown. Since both states have the same diabatic state, i. e. $|\psi_1\Phi_{(0,0,0)}\rangle$, they have the same global nodal structure, i. e. two regions of large probability to find the particles separated from each other, away from the diagonal $z_1 = z_2$. This can also be seen considering the mean radial density

$$\bar{r} = \int_0^\infty dr r \rho(r). \quad (24)$$

which is a measure for the mean distance of the particles. In Eq. (24),

$$\rho(r) = r^2 \int dV_{\mathbf{R}} d\Omega_{\mathbf{r}} |\Psi(\mathbf{r}, \mathbf{R})|^2 \quad (25)$$

is the radial pair density where $\Psi(\mathbf{r}, \mathbf{R})$ denotes the full six-dimensional wavefunction of the system, $dV_{\mathbf{R}}$ is the c.m. volume element and $d\Omega_{\mathbf{r}}$ is the angular volume element of the rel. motion. For the trap states of Fig. 7 the radial pair density is shown in Fig. 8. The large probability for the particles to be off-diagonal in Fig. 7 are clearly reflected. This can be quantified by the mean radial distance which is $\bar{r}_i = 3.95 d_y = 1.25 d_z$ at $d_y/a = 1.42$ and

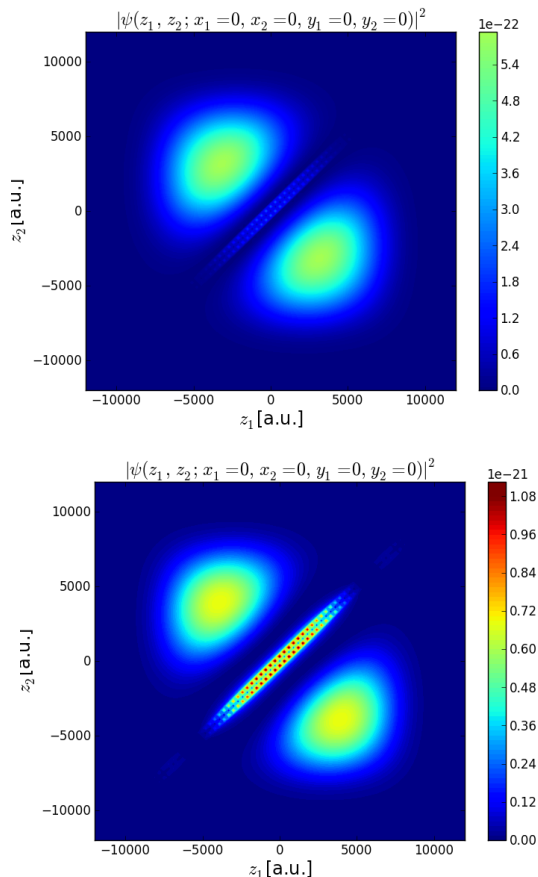


Figure 7. (Color online) Cuts along the elongated z -direction ($|\Psi(z_1, z_2; x_1 = x_2 = y_1 = y_2 = 0)|^2$) through the full six-dimensional *ab initio* wavefunction.

Upper part: The ground trap state diabatically described by $|\psi_1 \Phi_{(0,0,0)}\rangle$ at $d_y/a = 1.42$.

Lower part: The ground trap state diabatically described by $|\psi_1 \Phi_{(0,0,0)}\rangle$ at $d_y/a = -1.2$.

(For both plots an identical color code has been used).

$\bar{r}_l = 4.56 d_y = 1.44 d_z$ at $d_y/a = -1.2$. Hence, the mean distance of the trap state is on the order of the longitudinal trap length $d_z = 291$ nm which reflects the elongated shape of the confinement.

In the region of interaction a strong and small-scale nodal structure is visible close to the diagonal $z_1 = z_2$ where both particles are close to each other. The nodal structure is also visible in the inset of the radial pair-density plot which shows $\rho(r)$ for small r . In this region, the Born-Oppenheimer interaction potential possesses a deep minimum (compared to the energy scale of the trapping potential) which supports many bound states leading to the rich nodal structure.

In Fig. 9 cuts through the bound-state densities are shown. In both states, the particles only occupy regions where they are very close to each other, i. e. close to the diagonal $z_1 = z_2$. The bound state at $d_y/a = 1.42$ (upper panel in Fig. 9) has no c.m. excitation in the z direction.

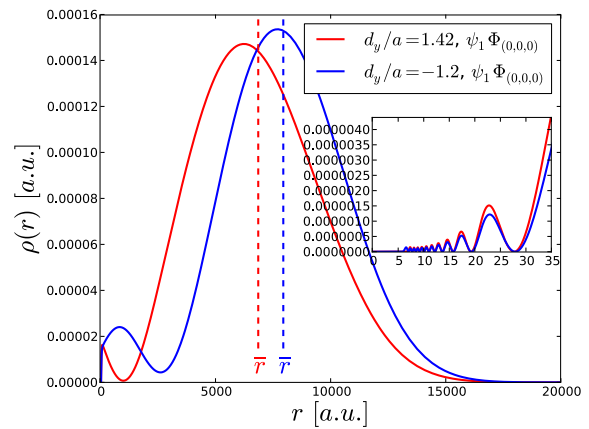


Figure 8. (Color online) Radial pair density of the first trap state for different values of the s -wave scattering length.

Hence, no zeros (nodes) are visible in the density (wavefunction) in scales of the trap length. Of course, the many small-scale oscillations in the bound-state regime stemming from the deep Born-Oppenheimer interaction potential are still present. The bound state at $d_y/a = -1.2$ shows four large-scale nodes along the z direction which is due to the $(0, 0, 4)$ c.m. excitation of this bound state.

At the transversally excited resonance, at $d_y/a = 1.42$, see Fig. 2, the atoms in the bound state which can be approximated by $|\psi_{(b)} \Phi_{(2,0,0)}\rangle$ have a mean distance of $\bar{r}_b = 0.29 d_y$, i. e. it is small compared to the confinement length in the tight y direction. This demonstrates the strong binding of the atoms. Away from the $(0, 0, 4)$ resonance, at $d_y/a = -1.2$, the atoms in the bound state have a mean distance of $\bar{r}_b = 1.01 d_y = 92.9$ nm, i. e. it is on the order of the trap length in the tightly confined direction.

An interesting question is whether the bound state at the $(0, 0, 4)$ resonance at $d_y/a = -1.2$ has enough bound character to trigger molecule formation and subsequent losses in a many-body system.

In [12] a molecule formation was observed experimentally at the resonance where the atoms in the bound state had a mean radial distance of $\bar{r}_b = 140$ nm. This is even larger than the value of $\bar{r}_b = 96.8$ nm at the $(0, 0, 4)$ resonance. Hence, a molecule formation with subsequent processes is also expected at this resonance.

IX. CONCLUSION

Experiments [7, 12] have demonstrated that inelastic confinement induced-resonances can influence the stability of an ultracold quantum gas and can be adopted to create molecules fully coherently. The resonances detected so far were measured in a strongly anisotropic confinement at large positive values of the s -wave scattering length. In fact, it has been demonstrated that they were all of a special kind, namely the ones excited

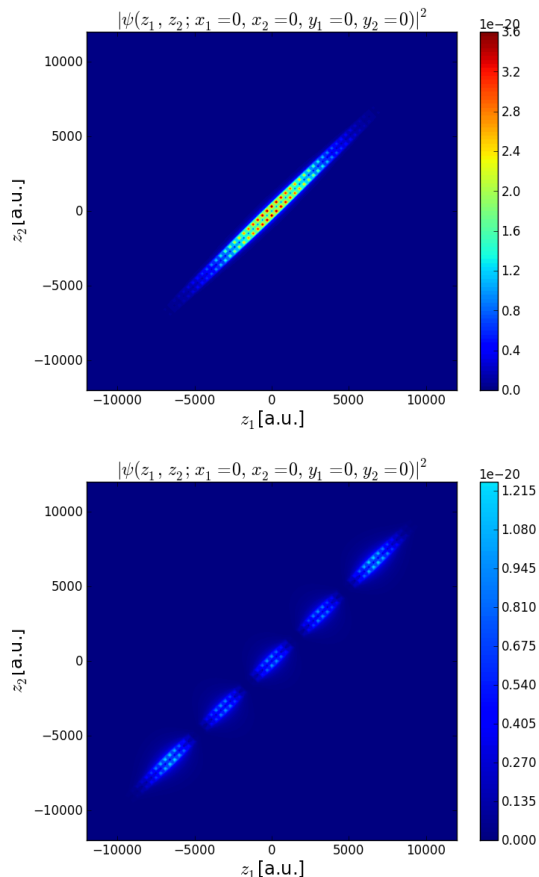


Figure 9. (Color online) Cuts along the elongated z -direction ($|\Psi(z_1, z_2; x_1 = x_2 = y_1 = y_2 = 0)|^2$) through the full six-dimensional *ab initio* wavefunction.

Upper part: The c.m. excited bound state diabatically described by $|\psi_b \Phi_{(2,0,0)}\rangle$ at $d_y/a = 1.42$.

Lower part: The c.m. excited bound state diabatically described by $|\psi_b \Phi_{(0,0,4)}\rangle$ at $d_y/a = -1.2$.

(For both plots an identical color code has been used.)

in the strongly confined direction. In the present work it is demonstrated that also resonances in the weakly confined direction occur. Models are introduced to describe the resonance position and the coupling strength of, in principle, all c.m.-rel. coupling resonances of a system of two ultracold atoms.

A study of the most pronounced resonances is performed for a variation of the external confinement. The lowest-order resonance in the strongly confined direction(s) and the next to leading order resonances in the weakly confined direction(s) are discussed in the transition of an almost isotropic 3D confinement to a quasi-1D (cigar-shaped) and a quasi-2D (pancake-shaped) confinement. While the position and the coupling strength of the resonance(s) excited in the strongly confined direction converge monotonically to a constant (non-zero) value for an increasing anisotropy, the position of the resonance(s) excited in the weakly confined direction fade

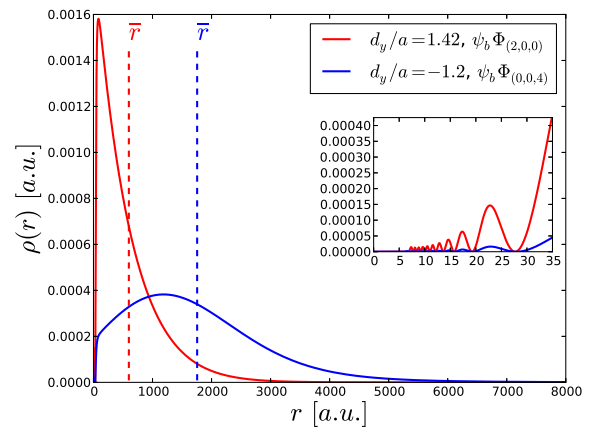


Figure 10. (Color online) Radial density of the c.m. excited bound states.

away to negative infinity for an increasing anisotropy and the coupling strength approaches zero. These resonances show a maximum in the coupling strength for intermediate anisotropies.

The models are discussed in comparison to *ab initio* calculations. In the transition to a cigar-shaped confinement geometry, the resonance positions are described accurately by the model C. The coupling strength is described quantitatively correct by model 1 for the resonances in the strongly confined direction and qualitatively correct for the resonance in the weakly confined direction.

In the transition to a pancake-shaped geometry, the resonance position of the resonance with an excitation in the strongly confined direction is described quantitatively accurate. For the resonances in the weakly confined direction, the accuracy for different anisotropies depends on the used approximations. The coupling strengths are reproduced qualitatively by the model 2 except for large anisotropies. For the latter the model 2 faces limitations and results in negative coupling strengths.

A variation of the potential depth shows that the c.m.-rel. coupling can be increased by decreasing the potential depth. While the position of the resonances in a very shallow sextic potential is still described accurately by the model B, the values for the coupling strengths lose their accuracy, since the harmonic approximation of the wavefunctions the model is based on loses its validity. Therefore, while the discussed models provide a helpful guide, the full *ab initio* calculation remains indispensable for highly precise quantitative predictions or for describing properly some trap geometries.

The analysis of the wavefunctions involved in the resonances in a cigar-shaped potential demonstrates that molecule formation and subsequent losses are also expected for the resonance excited in the weakly confined direction. In this case they occur for large negative values of the s -wave scattering length. We hope that this type of resonance will soon be verified experimentally.

The study of inelastic CIR has demonstrated that one of the most fundamental and routinely adopted approximations in ultracold atomic quantum gases — the harmonic approximation — has to be abandoned in order to describe particle loss, heating, and molecule formation in a variety of experiments. In fact, the inelastic CIR can be tuned not only by a variation of the scattering length but alternatively by a modification of the confinement geometry. Hence, it might deliver a novel tool for ultracold-atom experiments to alter the interaction behavior by a variation of the external confinement in the vicinity of an inelastic CIR. This can be valuable in cases where the standard technique of using magnetic Feshbach

resonances may not be available, such as for earth-alkali atoms. Similar to a magnetic Feshbach resonance, at the inelastic CIR the association of molecules can be tuned fully coherently.

ACKNOWLEDGMENTS

The authors gratefully acknowledge financial support from the *Studienstiftung des deutschen Volkes* and the *Fonds der Chemischen Industrie*.

-
- [1] T. Busch, B.-G. Englert, K. Rzazewski, and M. Wilkens, *Found. Phys.* **28**, 549 (1998).
- [2] T. Stöferle, H. Moritz, K. Günter, M. Köhl, and T. Esslinger, *Phys. Rev. Lett.* **96**, 030401 (2006).
- [3] F. Deuretzbacher, K. Plassmeier, D. Pfannkuche, F. Werner, C. Ospelkaus, S. Ospelkaus, K. Sengstock, and K. Bongs, *Phys. Rev. A* **77**, 032726 (2008).
- [4] S. Grishkevich and A. Saenz, *Phys. Rev. A* **80**, 013403 (2009).
- [5] S. Sala, P.-I. Schneider, and A. Saenz, *Phys. Rev. Lett.* **109**, 073201 (2012).
- [6] S.-G. Peng, H. Hu, X.-J. Liu, and P. D. Drummond, *Phys. Rev. A* **84**, 043619 (2011).
- [7] E. Haller, M. J. Mark, R. Hart, J. G. Danzl, L. Reichsöllner, V. Melezhik, P. Schmelcher, and H.-C. Nägerl, *Phys. Rev. Lett.* **104**, 153203 (2010).
- [8] M. Olshanii, *Phys. Rev. Lett.* **81**, 938 (1998).
- [9] T. Bergeman, M. G. Moore, and M. Olshanii, *Phys. Rev. Lett.* **91**, 163201 (2003).
- [10] V. S. Melezhik and P. Schmelcher, *Phys. Rev. A* **84**, 042712 (2011).
- [11] V. Dunjko, M. G. Moore, T. Bergeman, and M. Olshanii, in *Advances in Atomic, Molecular, and Optical Physics*, Vol. 60 (Academic Press, 2011) pp. 461 – 510.
- [12] S. Sala, G. Zürn, T. Lompe, A.N. Wenz, S. Murmann, F. Serwane, S. Jochim, and A. Saenz, *Phys. Rev. Lett.* **110**, 203202 (2013).
- [13] B. Schulz, S. Sala, and A. Saenz, *New J. Phys.* **17**, 065002 (2015).
- [14] M. Troppenz, S. Sala, P.-I. Schneider, and A. Saenz, “Inelastic confinement-induced resonances in quantum dots,” (2015), arXiv:1509.01159.
- [15] E. L. Bolda, E. Tiesinga, and P. S. Julienne, *Phys. Rev. A* **71**, 033404 (2005).
- [16] V. Peano, M. Thorwart, C. Mora, and R. Egger, *New J. Phys.* **7**, 192 (2005).
- [17] S. Grishkevich and A. Saenz, *Phys. Rev. A* **76**, 022704 (2007).
- [18] V. Melezhik and P. Schmelcher, *New Journal of Physics* **11**, 073031 (2009).
- [19] P.-I. Schneider, S. Grishkevich, and A. Saenz, *Phys. Rev. A* **80**, 013404 (2009).
- [20] J. P. Kestner and L.-M. Duan, *New J. Phys.* **12**, 053016 (2010).
- [21] G. Lamporesi, J. Catani, G. Barontini, Y. Nishida, M. Inguscio, and F. Minardi, *Phys. Rev. Lett.* **104**, 153202 (2010).
- [22] M. Valiente and K. Mølmer, *Phys. Rev. A* **84**, 053628 (2011).
- [23] Z. Idziaszek and T. Calarco, *Phys. Rev. A* **74**, 022712 (2006).
- [24] S. Grishkevich, S. Sala, and A. Saenz, *Phys. Rev. A* **84**, 062710 (2011).
- [25] In more detail: Compared to the model presented in [5], the here presented model uses a different formula for the bound-state energy and the anharmonic corrections are treated differently. These changes extend substantially the applicability of the model. The coupling strengths were not treated explicitly in previous works.
- [26] I. Bloch, *Nat. Phys.* **1**, 23 (2005).
- [27] J.-J. Liang and C. Zhang, *Phys. Scr.* **77**, 025302 (2008).
- [28] S.-G. Peng, S. S. Bohloul, X.-J. Liu, H. Hu, and P. D. Drummond, *Phys. Rev. A* **82**, 063633 (2010).
- [29] J. Förster, A. Saenz, and U. Wolff, *Phys. Rev. E* **86**, 016701 (2012).
- [30] S. Grishkevich, P.-I. Schneider, Y. V. Vanne, and A. Saenz, *Phys. Rev. A* **81**, 022719 (2010).
- [31] The reason why the (0, 0, 4) resonance is much stronger than the, e.g., (0, 2, 2) resonance in Fig. 2 compared to the Table I is the different confinement geometry, strongly elongated against almost isotropic, respectively.
- [32] M. J. Mark, S. Sala, F. Meinert, K. Lauber, E. Kirilov, A. Saenz, and H.-C. Nägerl, “Observation of Ultranarrow Feshbach Resonances and Inelastic Confinement-Induced Resonances in a Three Dimensional Optical Lattice,” (2015), in preparation.
- [33] I. Gradshteyn and I. Ryzhik, *Table of Integrals, Series, and Products* (Academic Press, 2007).

X. APPENDIX

A. 2-Channel model

To obtain the resonance position and coupling strength from *ab initio* calculations, a two-channel model is fitted to the eigenenergy spectrum in the vicinity of the investigated resonance. There are two diabatic states, the trap state $|t\rangle$ and the bound state $|b\rangle$ with diabatic energies E_t

and E_b . Introducing a coupling W between these states, the Hamiltonian matrix

$$H = \begin{pmatrix} E_t & W \\ W & E_b \end{pmatrix} \quad (26)$$

is obtained. A diagonalization of this matrix by a linear transformation $H_d = U^{-1}HU$, where U consists of the eigenvectors of the diagonal matrix H_d , leads to the energies E_1 and E_2 of the adiabatic states which are known from the *ab initio* calculations. Assuming that the adiabatic states are linear in the vicinity of the avoided crossing, i. e. $E_t = ax + b$ and $E_b = cx + d$ (where $x = \frac{d_y}{a}$), the coefficients a, b, c, d and the coupling W can be obtained by a minimization $\|U^{-1}HU - H_d\|$. The position of the resonance is then easily obtained from the crossing point of $E_t(x)$ and $E_b(x)$.

B. Perturbation Theory

For a correction of the resonance positions in the model B, the energies of the c.m. trap states in the sextic potential are treated within first-order perturbation theory. Since the c.m. Hamiltonian separates, it is sufficient to evaluate the 1D Hamiltonians. The unperturbed system is the 1D harmonic oscillator for which the wavefunctions are given in Eq. (15). The anharmonic terms of the sextic potential

$$V_j^{(a)}(R_j) = -\frac{1}{24} \frac{\hbar\omega_j}{V_j} R_j^4 + \frac{1}{720} \frac{\hbar^2\omega_j^2}{V_j^2} R_j^6 \quad (27)$$

are treated as a perturbation. Here the potential is written in dimensionless units of energies in $\hbar\omega_j$ and lengths

in $\sqrt{\frac{\hbar}{M\omega_j}}$, where $M = 2m$. For simplicity, only a single spatial direction is considered in the following and the subscript j is omitted. The first-order energy correction is determined by

$$E_n^{(a)} = \int_{-\infty}^{\infty} dR |\psi(R)|^2 V^{(a)}(R). \quad (28)$$

An exact expression for the integral of a triple product of Hermite polynomials and a Gaussian is known to be [33]

$$\int_{-\infty}^{\infty} dx e^{-x^2} H_k(x) H_n(x) H_m(x) = \frac{2^{\frac{m+n+k}{2}} \sqrt{\pi} k! n! m!}{(s-k)! (s-n)! (s-m)!} \quad (29)$$

where $2s = n + k + m$ must be even. To make use of this formula the R^4 and R^6 terms in $V^{(a)}$ need to be expressed in Hermite polynomials. For example,

$$R^4 = \frac{1}{16} H_4(R) + \frac{3}{4} H_2(R) + \frac{3}{4} H_0(R). \quad (30)$$

Inserting the expressions for R^4 and R^6 into the integral in Eq. (28), splitting the integrals, and evaluating each with formula Eq. (29) yields

$$E_n^{(a)} = -\frac{1}{1152 V^2} \left[36 (2n^2 + 2n + 1) V \hbar^2 \omega^2 - (4n^3 + 6n^2 + 8n + 3) \hbar^3 \omega^3 \right]. \quad (31)$$

To determine the 3D perturbative energies $E_n = \sum_{j=x,y,z} E_{n,j}^{(h)} + E_{n,j}^{(a)}$ of the sextic potential the anharmonic energy corrections $E_{n,j}^{(a)}$ of the three spatial directions and the corresponding harmonic oscillator energies $E_n^{(h)} = \hbar\omega_j (n + \frac{1}{2})$ need to be added up.